ACS OMEGA

http://pubs.acs.org/journal/acsodf

Article

Natural Fracture Development Characteristics and Their Relationship with Gas Contents—A Case Study of Wufeng–Longmaxi Formation in Luzhou Area, Southern Sichuan Basin, China

Shun He, Qirong Qin,* Zhangjin Qin, and Jiling Zhou

Cite This: *ACS Omega* 2022, 7, 34066–34079

Read Online

ACCESS | Metrics & More | Article Recommendations

ABSTRACT: Natural fractures are critical factors that should be considered in shale reservoir evaluation, storage condition analysis, horizontal well design, and fracturing stimulation, which also play a non-negligible role in the occurrence state of shale gas in the reservoir. This paper discussed the influence of fracture development on gas-bearing properties based on the analysis results of core observation, scanning electron microscopy, mineral composition, and gas-bearing properties after the development characteristics of fractures and their longitudinal variation law were clarified. In this way, the development characteristics of organic-rich marine shale fractures in the Longmaxi Formation in the 203 well area of the Luzhou member of the Sichuan Basin and their effects on the gas-bearing properties can be analyzed. The results show that the Longmaxi Formation shale develops shear fractures, extensional fractures of tectonic origin, bedding fractures, dissolution fractures, and abnormally high-pressure fractures of nonstructural origin. Specifically, interlayer fractures, intercrystalline fractures, organic matter contraction fractures, and fractures between clay layers are microfractures. Fracture development is characterized by short longitudinal extension, small opening, high degrees of composite filling, and large density changes, with calcite and pyrite as the filling materials. The fracture density has a "three-stage" variation pattern longitudinally, and the bottom is dominated by thin siliceous shale development, together with a small amount of shale mixed with calcareous and calcareous materials. Moreover, the fracture is dominated by "splitting" and "shearing" failure, crossing stratification with the fracture density. The highest fracture density was found in the 2 sub-layer, featuring the joint development of horizontal and vertical fractures, which form the mesh fracture system through mutual cutting and restriction. The lithofacies in the 4 sub-layer are dominated by clay siliceous shale with a small amount of mixed shale of calcareous and siliceous materials. The formation of fractures always expands along the lamellation direction, which has concentrated development members of top and bottom fractures, with the development of horizontal fractures dominated and vertical fractures less developed. Furthermore, a synergistic effect can be found among the total organic carbon (TOC) content, fracture density, and gas-bearing property of the shale in Longmaxi Formation. It is worth noting that a high TOC content and siliceous content are conducive to the formation of microfractures, while the development of fracture contributes to the total gas-bearing property, especially to the increase in free gas content. To be concrete, the free gas content in the fracture development member accounts for more than 55% of the total gas content, thanks to a channel provided by fractures for the desorption of shale gas.

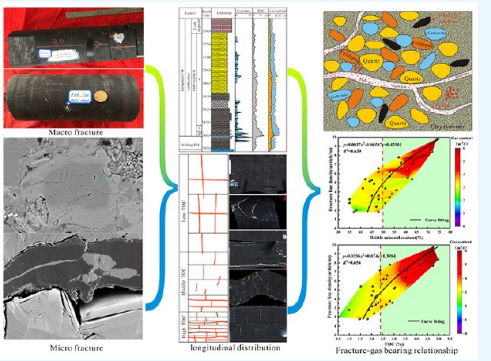

1. INTRODUCTION

Horizontal wells and hydraulic fracturing technology have enabled the commercial development of shale gas. With production increased year by year, shale gas becomes the most important composition of unconventional oil and gas exploration. Meanwhile, its exploration and development march into the "deeper, older, and wider"domain.[1−3] The Wufeng–Longmaxi Formation shale in the southern Sichuan Basin has become a major stratum for shale gas exploration and development because of its high total organic carbon (TOC) content, highly brittle mineral content, high maturity, large effective thickness, and contiguous distribution.[4,5] Shale is widely perceived as combining "source, reservoir, and coverage" due to its features of "low porosity and low-to-extra-low permeability".[6,7] In addition, the free state occurring in pores,

Received: May 27, 2022
Accepted: September 5, 2022
Published: September 14, 2022

https://doi.org/10.1021/acsomega.2c03318
ACS Omega 2022, 7, 34066–34079

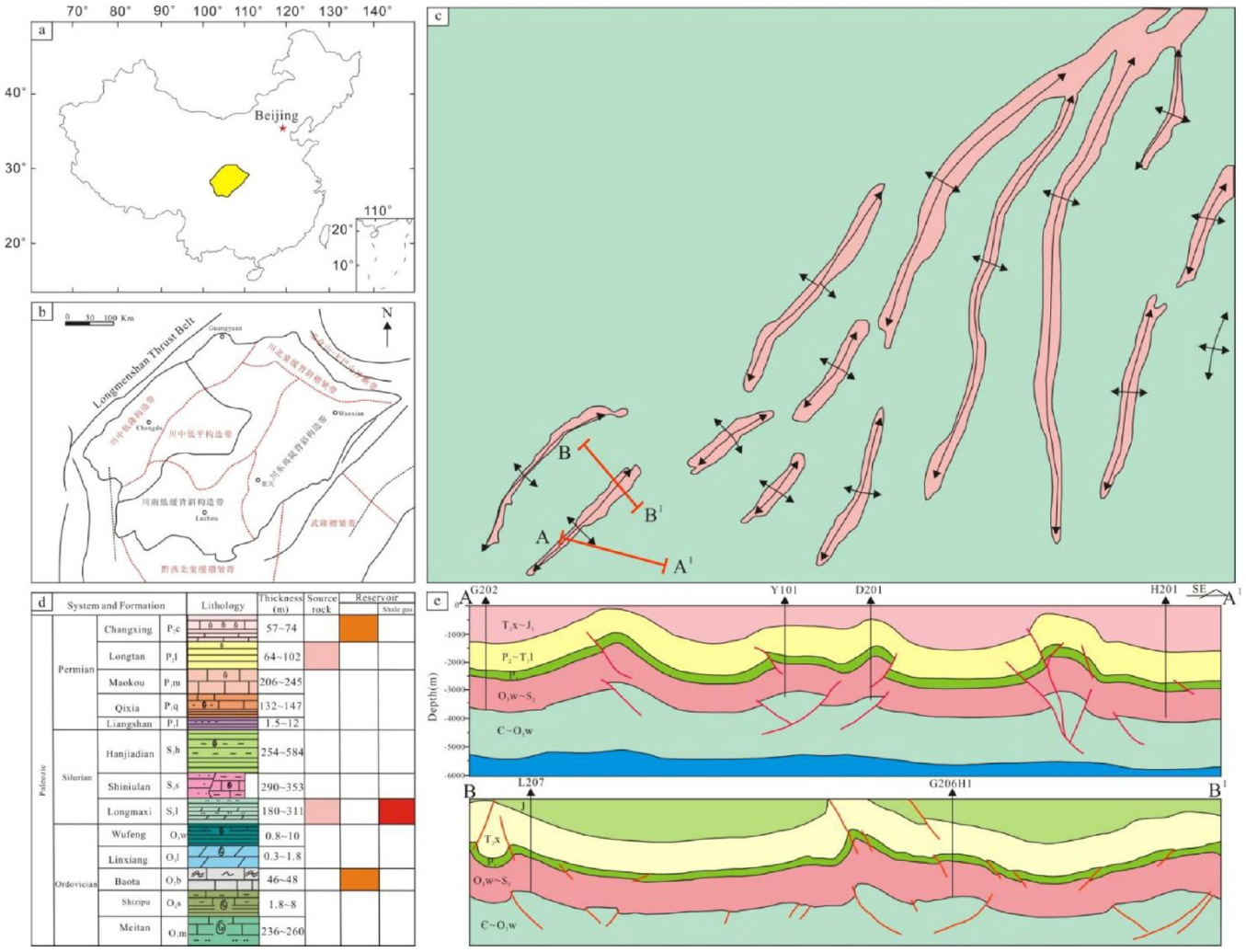

Figure 1. Geological overview and comprehensive histogram of L203 well area: (a) geographical location of the Sichuan Basin; (b) structural division of the Sichuan Basin; (c) characteristics of surface folds in Luzhou area; (d) stratigraphic comprehensive histogram; (e) typical crossing well profile.

adsorbed on the surfaces of organic matters and mineral particles in the adsorbed state, and a small amount of dissolved state are the occurrence states of hydrocarbon gas in shale.[8−10]

Natural fractures play pivotal roles in the shale storage space, preservation conditions, and the morphology and expansion form of artificial fracture networks during fracturing and development, according to actual results of shale gas exploration in the Appalachian Basin of the United States and the Sichuan Basin of China.[11−13] Hence, the development of natural fractures should be considered in geological exploration of shale gas, drilling direction design of horizontal wells, and hydraulic fracturing methods.[14] For reservoirs, unfilled fractures can also provide channels for the migration of shale gas to increase the effectiveness of shale reservoirs apart from being effective reservoir spaces.[8,15−17] Regarding the preservation conditions, the self-closed property of shale might be destroyed by the excessively developed fractures, leading to vertical dissipation of shale gas. Fractures are tectonic weak surfaces that naturally occur,[18−20] which are expanded first in the hydraulic fracturing treatment of reservoirs, affecting the formation of artificial fracture networks.[16,21,22] Also, more natural fractures are expected to drill in the drilling process of horizontal wells during drill design. This is because of more complex fracture network systems that are easily formed in the fracturing process, contributing to the improved effect of reservoir fracturing treatment.[23] Natural fractures become one of the critical factors controlling the migration, accumulation, and high yield of hydrocarbon gas in shale to some extent,[24] and the study on the spatial distribution of the natural fracture system is a prerequisite for the exploration of shale gas reservoirs.[25,26] Many scholars have focused on the research concerning the characteristics of natural fractures, plane distribution, elf-closed property, and the effect of the fracturing process on the complexity of the artificial fracture network with the on-going development of shale gas.[27−29]

The 203 well area in the Luzhou block is located at a complex tectonic environment in the Yongchuan broom-like tectonic belt of the southern Sichuan Basin. The Wufeng−Longmaxi Formation shale is buried mostly below 3500 m.[30] Specifically, the sedimentary environment of shale of the Wufeng−Longmaxi Formation (O_3w-S_1l), TOC content, thermal evolution degree, plane distribution, and paleo-tectonic stress field were analyzed in the preliminary study, proving that there are abundant shale gas resources in the Wufeng−Longmaxi Formation of the Luzhou block, presenting a great exploration prospect.[31] The formed shale deposition has a complex tectonic environment as it was affected by multistage tectonic movements such as the late Indosinian movement, the late Yanshan movement, and the

https://doi.org/10.1021/acsomega.2c03318
ACS Omega 2022, 7, 34066−34079

Himalayan movement. The development results of existing shale gas wells show that there are obvious differences in the productivity of single wells in the Luzhou block. The test productivity of Well L203 in the syncline area is 1.379 million cubic meters per day, which is the highest in the study area, and the test productivity of Well L207 is 306,300 cubic meters per day, while Well Yang 203H2, which is also located in the syncline area, has a single well productivity of 150,000 cubic meters per day, and Ti 201-H1 has a tested productivity of only 50,000 cubic meters per day. Total gas content and different occurrence states of shale in the fracture developed and underdeveloped members are remarkably different due to the effect of development of microfractures. Fracture characteristics and their effects on gas-bearing properties were rarely studied due to the lack of outcrops and early drilling data. In recent years, the continuous development of deep shale gas and the increase of drilling cores and logging data have provided favorable conditions for studying their relationship. Focusing on the Wufeng−Longmaxi Formation in Wells L205 and L208, this paper analyzed the development characteristics of shale fractures in the Wufeng−Longmaxi Formation, longitudinal changes, and the correspondence to changes in mineral components based on core and field-emission scanning electron microscopy (FE-SEM) observations together with logging data. Moreover, the relationship among fracture development degrees, changes in mineral components, and gas-bearing properties of shale was also discussed in an attempt to provide a theoretical basis and reference for the exploration and development of deep shale gas in the Luzhou block and other areas.

2. GEOLOGICAL SETTING

Sichuan Basin located in the northwestern region of the Upper Yangtze Craton is a large-scale superimposed basin developed from sedimentation on the craton and also one of the most important gas-producing basins in China.[10,30] Surrounded by Qiyue Mountain, Daba Mountain, Longmen Mountain, and Dalou Mountain, its tectonic pattern is characterized by uplift in the middle, depression in the south, and intensive folds in the east and west (Figure 1a,b).[5,8,32] The 203 well area of the Luzhou block is located in Luzhou city, Sichuan Province, and structurally located in the south of the Yongchuan broom-like tectonic belt, which is the junction areas of the paleo-uplift-middle-slope gentle belt in central Sichuan, the paleo-middle-slope low-fold belt in southwestern Sichuan, and the ancient depression-middle-uplift low-steep belt in southern Sichuan, China.[33] It is composed of some areas of Yundingchang structure, Gufoshan structure, Tiziya structure, tide structure, Longdongping structure, and Xindianzi structure. Moreover, the structure of the study area is characterized by torsion with the structural axis presenting in the NE−EN direction, featuring convergence in the north and scattering in the south (Figure 1c).[34] The anticline in the study area is narrow and long with wide and gentle syncline. Various anticlines are presented as being high in the north and low in the south. The sandstone of the Xujiahe Formation is the oldest stratum exposed at the anticlinal core (Figure 1e), and the sandstone of Shaximiao Formation is the outcropped stratum in the syncline.

Early subsidence accompanied by short-term uplift and late sustained uplift can be observed in the Luzhou area,[35] presenting complete stratigraphic development. The formation of organic-rich shale in the Wufeng−Longmaxi Formation is directly related to the global transgression event in the Late Ordovician-Early Silurian.[36] A geographical pattern of "one depression in-between two uplifts" was formed under the influences of the Jiangnan-Xuefeng uplift and the Middle Guizhou paleo-uplift. As a result, the circulation of sedimentary water bodies was blocked, leading to the formation of reduced sedimentary water bodies that were occluded.[37] The Longmaxi Formation inherited the sedimentary environment in the late Ordovician period during the early Silurian period. The sedimentary substrate was characterized by being low in the northwest and high in the southeast. Meanwhile, the deepened sedimentary water body in the Luzhou area is to develop the blacked organic-rich shale in the deep shelf environment. The organic matter content of the shale in the upper Longmaxi Formation was decreased with the increased argillaceous and sandy content as the global sea level dropped, the sedimentary water became shallow, and terrigenous debris continuously input.[38] The Longmaxi Formation can be split into Long 1 Member (S_1l^1), Long 2 Member (S_1l^2), and Long 3 Member (S_1l^3) from bottom to top, which develop black shale, dark gray siltstone mixed with silty mudstone, and dark gray siltstone, respectively (Figure 1d).[38] Of which, the S_1l^1 is composed of two sub-members. Bottom 1 sub-member has high siliceous organic-rich shale that is the main development stratum at this stage. The shale at the Longmaxi Formation forms argillaceous limestone upward and is conformable contact in the shale of Ordovician Wufeng Formation downward. The thickness of shale is between 480 and 650 m, while the thickness of high-quality shale is more than 55 m. Type I organic kerogen dominated, which is in the high-over-mature dry gas production stage. The porosity and permeability of the shale matrix are between 0.84∼3.87% and 0.034∼0.15 mD, respectively, while the fractures porosity and fractures permeability of shale are between 1.59∼7.22% and 2.58∼138 mD, respectively.

3. SAMPLES AND METHODS

The development characteristics of fractures and their relationship with gas-bearing properties were mainly discussed by means of geological analysis and experimental testing in this study. Geological analysis mainly includes core fracture observation, statistics, logging data analysis, experimental methods mainly through scanning electron microscopy microscopic fracture observation, and whole rock "X" diffraction.

3.1. Geological Measure and Data Analyses. Due to the lack of corresponding field outcrops in the study area, the geological analysis is performed mainly through the observation of 158 m shale cores from the Wufeng−Longmaxi Formation of nine wells in the study area. The observation contents include the fracture type, width, dip angle, length, filling degree, filling object type, etc. The fracture linear density of a sub-member is calculated in units of small layers, and the gas content of shale is calculated by polynomial regression through logging curves.

3.2. Experimental Tests. *3.2.1. Whole Rock Mineral Composition.* Shale mineral components were obtained by whole-rock "X" diffraction experiments. The test samples were fresh samples from the cores. The experimental instrument was an X'Pert MPD PRO X-ray diffractometer produced by PANalytical Corporation of the Netherlands. The sample was washed with high-pressure air to remove surface impurities before the test, and the sample was manually broken. Then, 5−6 g of broken sample was selected and placed in an agate grinder, and the sample was ground to about 300 mesh for the XRD test. During the experiment, the weight of the powder sample was kept above 50 mg, the voltage of the instrument was gradually increased to 40 KV, and the current was 30 mA. Continuous

https://doi.org/10.1021/acsomega.2c03318
ACS Omega 2022, 7, 34066−34079

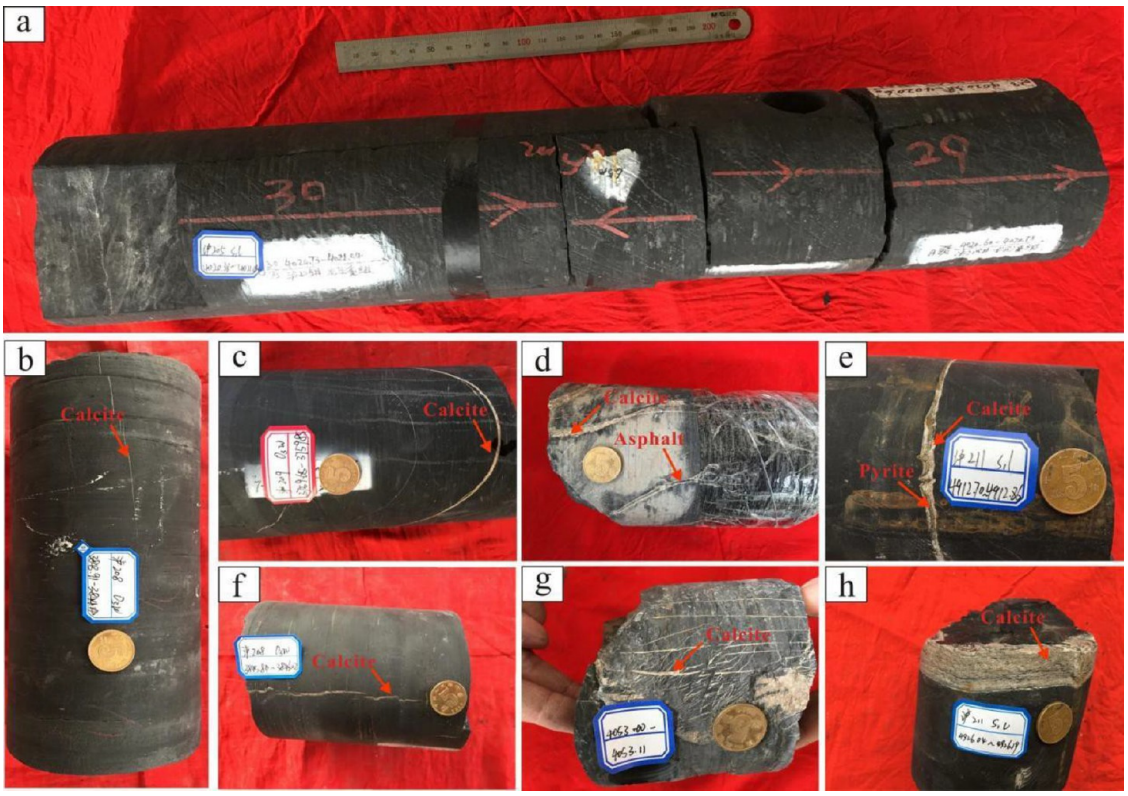

Figure 2. Core fracture characteristics of Wufeng−Longmaxi Formation in L203 Well area. (a) Upright shear fracture, unfilled, Well L205, 4020.38∼4021.04 m. (b) Upright shear fracture, filled with calcite, Well L208, 3843.91∼3844.14 m. (c) High-angle shear fracture, calcite fully filled, Well L209, 3759.65∼3759.85 m. (d) Tension fractures, fully filled with calcite and asphalt, Well L206, 4053.43∼4053.68 m. (e) Horizontal fractures, fully filled with calcite and asphalt, Well L211, 4912.70∼4912.86 m. (f) Tension fracture, filled with calcite, Well L208, 3845.84∼3846.026 m. (g) Abnormally high-pressure fracture, filled with calcite, Well L206, 4053.00∼4053.11 m. (h) Dissolution fracture, filled with calcite, Well L211, 4926.04∼4926.19 m.

scanning was carried out with the general qualitative analysis degree ($2\theta > 3°$), and the scanning step was 0.016 (°/step). The whole experiment was carried out at room temperature. The experimental procedure is in accordance with the Standard of the Petroleum and Natural Gas Industry of the People's Republic of China "X-ray Diffraction Analysis Method for Clay Minerals and Common Non-Clay Minerals in Sedimentary Rocks" SY/T 5163-2018.

3.2.2. TOC Content. The TOC content of the samples was tested with a CS230SH carbon and sulfur analyzer of leco company. Before the test, the samples were placed in deionized water, and the stains on the surface of shale were removed by ultrasonic waves, and the samples were dried at low temperatures. Then, the samples were ground to more than 150 mesh using an agate grinder, and the carbonate components in the samples were removed by excessive pickling of the powder samples. Oxygen with a purity of 99.5% was used as the carrier, and nitrogen was used as the power gas. Organic matter content was measured by a solid-state infrared absorption method.

3.2.3. FE-SEM Scan of Microstructures. The microscopic fractures were observed using an electron microscope. The experimental instrument was a Quanta 450 environmental scanning electron microscope produced by FEI Company in the United States. Fresh samples perpendicular to the plane were selected for experimental samples, which were mechanically cut into 10 mm × 10 mm in size. Argon ion focused beams were used to polish the sample surface, and the polished shale surface was ground to remove irregularities on the sample surface, and a carbon coating of about 15 nm was applied to increase the conductivity of the sample. During the experiment, the voltage and current were set at 10 KV and 15 nA, respectively.

4. DEVELOPMENTAL CHARACTERISTICS OF FRACTURES IN CORES

4.1. Fracture Types. Tectonic fractures and diagenetic fractures are jointly developed at the Wufeng (O_3w)−Longmaxi Formation (S_1l) shale in the study area, of which tectonic shear fractures as the major fracture type are developed in various lithologies with features such as the obvious directionality, straight and smooth fracture surface, long longitudinal extension, stable distribution, breaking shale mineral particles, and appearing in groups. A number of shear fractures with obvious differences generated in parallel arrangement are presented in the cross member of the core (Figure 2). Shear fractures can be divided into vertical and near-horizontal fractures as per the difference in dip angle. Vertical fractures, in general, are filled with calcite and pyrite. Transverse scratches and mirror surfaces can be apparently observed on the fracture surface, indicating that the shear fracture has a certain strike-slip property. The development of near-horizontal fractures is parallel to or intersecting with the plane at a small angle. Some horizontal fractures were filled with calcite, featuring obvious scratches, which formed a complex network system through interweaving with vertical fractures in some well sections. Extension fractures, in most cases, are developed at the bottom of the Wufeng Formation, featuring irregular fracture surface bending, large variations in fracture opening

https://doi.org/10.1021/acsomega.2c03318
ACS Omega 2022, 7, 34066−34079

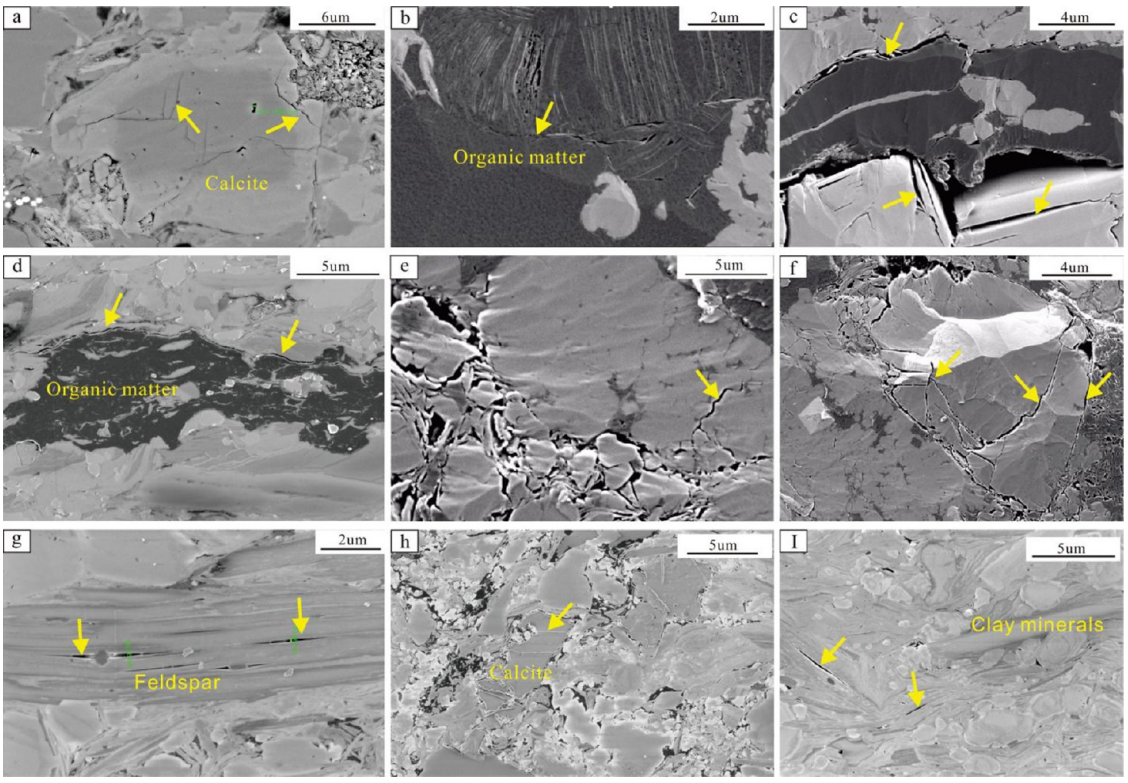

Figure 3. SEM photo of Wufeng−Longmaxi Formation shale. (a) Calcite intercrystalline fracture. (b) Microfractures developed in organic matter. (c) Edge seam between organic matter and clay minerals. (d) Edge seam between organic matter and clay minerals. (e) Calcite intercrystalline fracture. (f) Microcracks at the edge of contact between calcite and organic matter. (g) Feldspar dissolved fracture. (h) Microcracks on the edge of calcite. (i) Edge seam of the mica layer.

and occurrence, short longitudinal extension, and terminating mostly in horizontal fractures, which can be highly filled with calcite and asphalt. In general, bedding detachment fractures are parallel to the stratification. The fracture surface is straight and smooth with scratches or mirror surfaces, which are filled mostly with calcite or pyrite, featuring concentrated development at the bottom and top. Interlaminar fractures are the most common diagenetic fractures in the core, which are the result of the combined action of deposition, compaction, and diagenetic evolution, featuring development along bedding, short extension distance, small scale, and strong lateral connectivity. Such a fracture is of great significance in increasing the shale storage space, which can be also used as a channel for shale gas migration to improve the lateral permeability of shale. Abnormally high pressure is formed by abnormal fluid pressure and organic matter hydrocarbon generation pressurization. When the pressure exceeds the tensile strength of shale, abnormally high-pressure fractures will be formed. These fractures expand normally along the bedding plane, with limited development, short extension, significant variation in width, irregular shape, and lenticular or fibrous output. In general, it is filled with calcite. In the diagenesis process, dissolution fractures are formed by dissolving soluble mineral particles with fluid in the horizontal presentation, which are mostly filled with calcite with the width ranging from 1 to 3 mm.

4.2. Microscopic Characteristics of Fractures. Shale has lower matrix porosity and permeability in comparison to conventional reservoirs,[39] and microfractures are essential for the increase of effective pore storage and deep flow capacity.[40] A large number of microscopic fractures are developed in the Wufeng−Longmaxi shale, mostly in clay minerals and quartz, according to SEM results. These fractures are mostly non-structural fractures, including organic matter contraction fractures, clay mineral interlayer fractures, mineral intercrystalline fractures, and corrosion fracture. Organic matters in shale are distributed in points and clusters and are contracted in the process of sedimentary compaction and hydrocarbon generation evolution. Microfractures developed inside and isolated organic matter pores become the accumulation and migration channels of shale gas, with short extension distance of fractures and the opening degree below 50 nm. Edge fractures are formed at the contact of organic matter with clay minerals and siliceous minerals due to the hydrocarbon generation contraction of organic matters and the burial and dehydration of clay minerals, which are bending fractures with large differences in width, ranging from 20 to 200 nm. These unfilled fractures are favorable gathering place for shale gas. High content of clay minerals such as mica, illite and montmorillonite, etc. can be found in shale. The clay is mostly developed in sheets. Meanwhile, edge fractures can be developed between clay mineral sheets. These fractures are mainly developed along the clay mineral sheets, featuring wide in the middle of fractures, and thin at the edge. Quartz and feldspar minerals are highly brittle and prone to rupture, forming fractures in the later tectonic movement. Microscopically, complex and numerous fractures can be observed on the surface of quartz and feldspar mineral grains. The fracture surfaces are straight and extended long, intersecting the entire mineral grains. The mineral edge has a high degree of fracture, which can be developed as edge fractures at the contact with the clay mineral. Dissolution fractures were formed as the feldspar dissolved in the long-term burial diagenesis process, which were filled with pyrite. Meanwhile, a great amount of

https://doi.org/10.1021/acsomega.2c03318
ACS Omega 2022, 7, 34066−34079

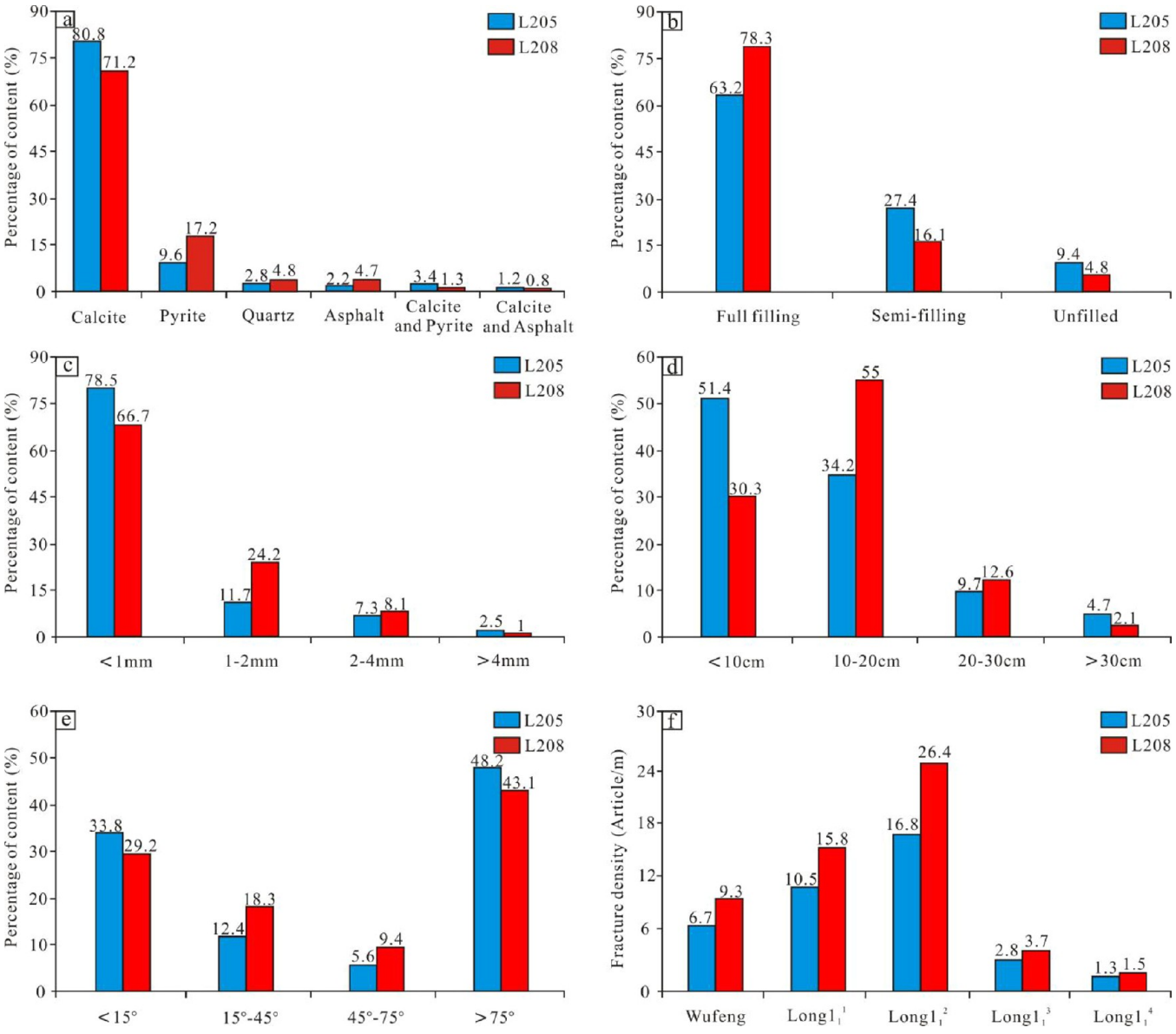

Figure 4. Statistics of fracture parameters in cores of S1l in Wells L205 and L208. (a) Histogram of filling type distribution. (b) Histogram of filling degree distribution. (c) Histogram of fracture opening degree distribution. (d) Histogram of fracture extension length distribution in the core. (e) Histogram of fracture dip angle distribution. (f) Histogram of fracture density distribution in different sublayers.

microfractures developed in the calcite intercrystalline and intracrystalline were found at the member with high calcite content. These thin and small fractures are extended along the cleavage surface, featuring a straight fracture surface, short extension distance, and small opening.

4.3. Characteristic Parameters of Core Fractures. The fracture filling degree is high according to the statistical results of characteristic parameters such as the fracture filling degree, filling material type, extension length, width, and dip angle in the cores of Wufeng−Longmaxi Formation. Combined with core immersion observation, the fully filled fractures, half-filled fractures, and unfilled fractures in Well L205 account for 63.2%, 27.4%, and merely 9.4% of the total number of fractures, respectively. By comparison, the fully filled fractures, half-filled fractures, and unfilled fractures in Well L208 are 78.3%, 16.1%, merely 4.8%, respectively, as shown in Figure 3b. Fracture filling is composed of single-mineral filling and multimineral mixed filling. Filling minerals incorporate calcite, pyrite, quartz, and asphalt, of which calcite filling is the main filling material, accounting for 80.8 and 71.2% of the total number of fractures, respectively, followed by pyrite, accounting for 9.6 and 17.2% of the total number of fractures. Quartz and bitumen are less filled. Besides, mixed fillings involve pyrite−calcite mixed filling and calcite−asphalt mixed filling, as shown in Figure 3a. The shale of the Wufeng−Longmaxi Formation is deeply buried. The core fractures of Well L205 and Well L208 are low-opening fractures with openings of less than 1 mm, accounting for 78.5 and 66.7% of the fractures, respectively; fractures with a width of 1−2 mm account for 11.7 and 24.2% of the total number of fracture, respectively; fractures with a width of 2−4 mm account for 7.3 and 8.1% of the total number of fractures, respectively; and fractures with a width of more than 4 mm account for 2.5 and 1% of the total number of fractures, respectively, as shown in Figure 3c.

Considering the longitudinal extension length of fractures, core fractures are dominated by small fractures. To be specific,

https://doi.org/10.1021/acsomega.2c03318
ACS Omega 2022, 7, 34066−34079

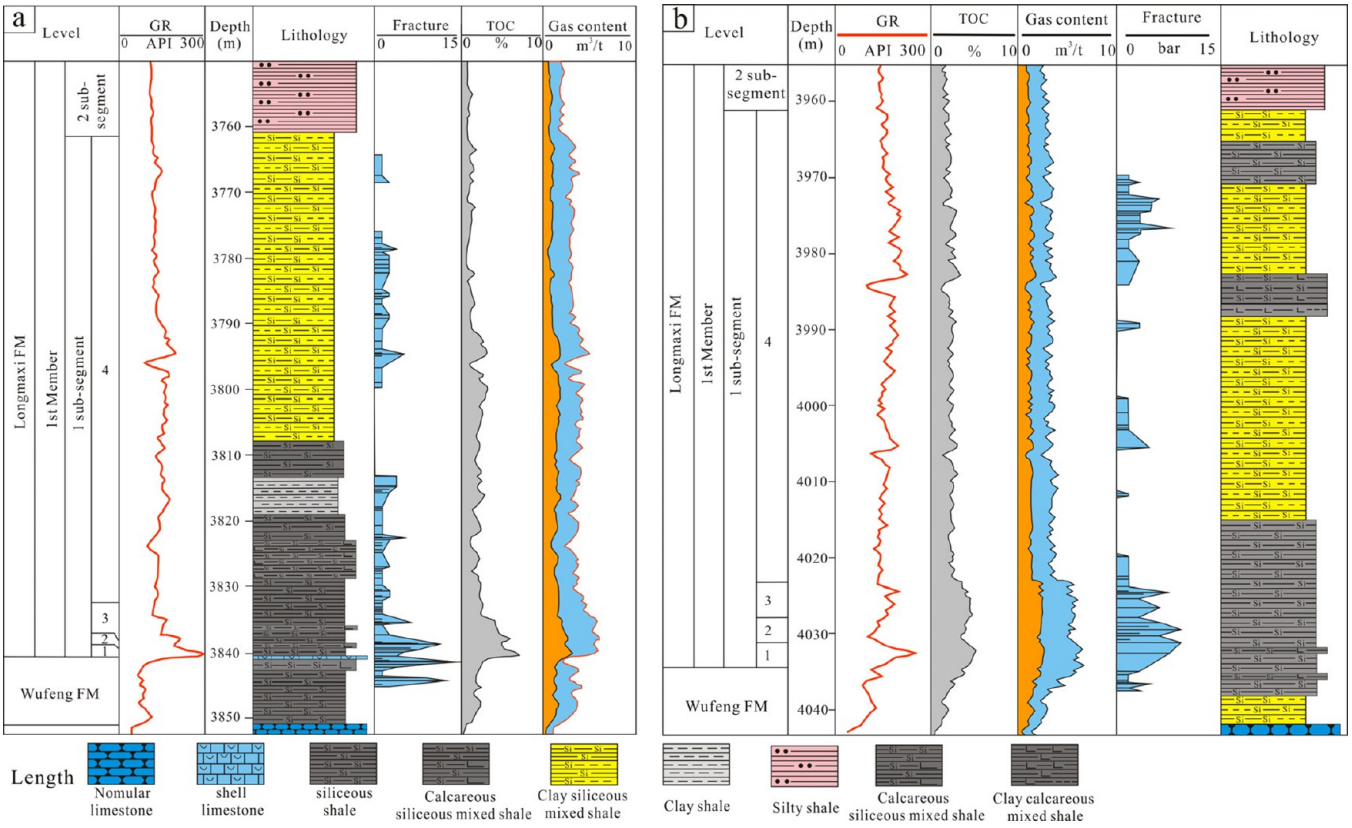

Figure 5. Longitudinal variation characteristics of fractures in Wells L208 and L205. (a) Histogram of longitudinal distribution of fractures in Well L205. (b) Histogram of longitudinal distribution of fractures in Well L208.

microfractures (L < 10 cm), small-scale fractures (10 < L < 20 cm), medium-sized fractures (20 < L < 30 cm), and large fractures (L > 30 cm) account for 51.4, 34.2, 9.7, and 4.7% of the total fractures in Well L205, respectively. Moreover, there are a small number of large straight-split fractures with a length of more than 1 m, as shown in Figure 2a. To be concrete, microfractures (L < 10 cm), small-scale fractures (10 < L < 20 cm), medium-sized fractures (20 < L < 30 cm), and large fractures (L > 30 cm) account for 30.3, 55, 12.6, and 2.1% of the total number of fractures in Well L208, as shown in Figure 4d. Fractures can be divided into horizontal fractures, low-angle fractures, high-angle fractures, and vertical fractures as per the differences in fracture dip angles. Vertical and horizontal fractures are mainly developed wells L205 and L208, of which vertical fractures account for 48.2 and 43.1% of the total number of fractures in Wells L205 and L208, respectively, and horizontal fractures account for 33.8 and 29.2% of the total number of fractures, respectively, and high-angle fractures and low-angle oblique fractures are less developed.

Fracture density is the main parameter to quantify the degree of fracture development, including linear density, areal density, and volume density.[41−44] The calculation formula is as follows:

$$\Gamma = \Delta n/\Delta L;\ P = \Delta l/\Delta S;\ T = \Delta S/\Delta V$$

In the formula, T is the bulk density of the fracture medium; ΔS is the unit volume; ΔV is half of the area of all the fracture surfaces in the unit volume. P is the crack surface density value; Δl is the sum of the lengths of crack impressions spread over the unit volume; ΔS is the unit volume; Γ is the crack line density value.

Combining the research requirements and the core fracture performance, we calculated the fracture line density by using the average number of fractures per unit length along the average normal vector of the core fractures. The results show that there are significant differences in the development of fracture density at different sub-layers (Figure 3d). Vertically, the fracture density is higher in the Wufeng Formation-1 sub-member in the 2 sub-layer and lower in 3 and 4 sub-layers. The highest fracture densities of both wells reached the maximum in the 2 sub-layer of the 1 sub-member (S_1l^1 sub-member) with 26.4 fractures/m in Well L208 and 16.8 fractures/m in Well L205, respectively, as shown in Figure 3f.

4.4. Longitudinal Variation Characteristics of Fractures. Fractures in Wells L205 and L208 are longitudinally distributed in a similar manner. Overall, the fracture density is varied in a trend of increasing−decreasing−increasing from the Wufeng Formation to the 4 sub-layer of the S_1l^1 sub-member. Moreover, two fracture concentrated development members can be observed at the bottom and the upper-middle ems of the 4 sub-layer. Fractures are divided into horizontal fractures and vertical fractures with 45° as the boundary for statistics, according to the well logging interpretation of fracture occurrence. Among them, Well L208 has a high fracture density with the Wufeng Formation developing thick layered siliceous shale of high ash content at the bottom and a fracture density of 9.3 fractures/m, which is dominated by small vertical fractures with horizontal fractures less developed. Fractures are developed in concentration within 2 m below the shell limestone. The fracture density of the 1 sub-layer in the S_1l^1 sub-member was 15.8 fractures/m, the horizontal and vertical fractures of which are 6.65 fractures/m and 9.15 fractures/m, respectively, with the

https://doi.org/10.1021/acsomega.2c03318
ACS Omega 2022, 7, 34066−34079

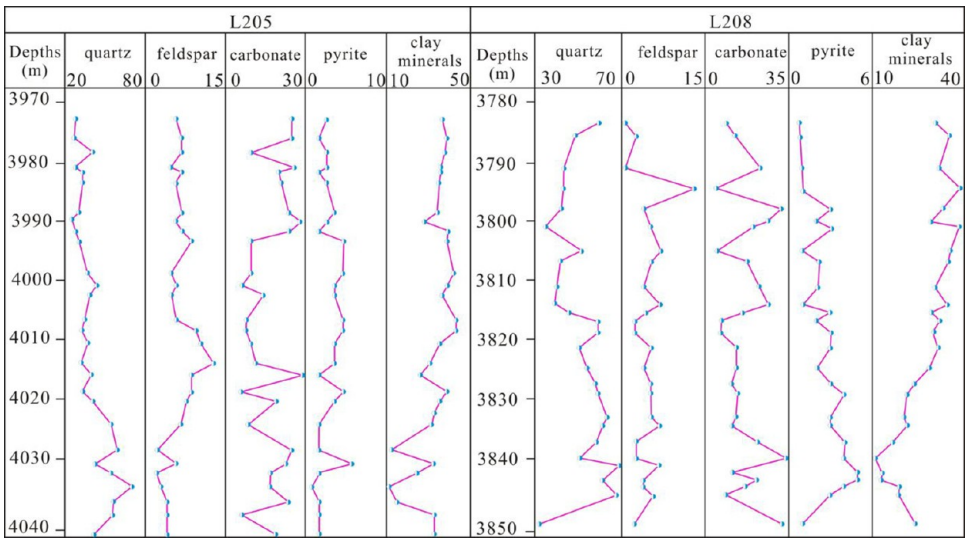

Figure 6. Variation characteristics of mineral contents in the shale of the Longmaxi Formation in Luzhou area.

highest fracture density in the 2 sub-layer, reaching 26.4 fractures/m. The thickness of the monolayer was thin with well-developed stratification and horizontal fractures. To be specific, the densities of horizontal and vertical fractures were 7.16 fractures/m and 19.24 fractures/m, respectively. The longitudinal extensions of fractures in 1 and 3 sub-layers resulted in the rising statistical density of the 2 sub-layer, presenting a significant cutting and restricting relationship. On this basis, a complex mesh fracture system can be generated. Fractures in the 3 sub-layer had decreased rapidly with density reaching 3.7 fractures/m, large thickness of the monolayer, and the domination of horizontal fractures developed. Fractures in the 4 sub-layer with large thickness and large numbers of fractures with a density of 1.5 fractures/m were developed vertically at the bottom and upper members of the 4 sub-layer in concentration. More precisely, siliceous shale, lime clay shale, and clay shale developed at the bottom were dominated by horizontal fractures, while the thick clay siliceous shale in the middle and upper members was dominated by the development of horizontal fractures, with a small number of vertical fractures. Hence, a simple fracture network was formed by the intersecting fractures. The fracture development degree of Well L205 was lower than that of Well L208 as a whole. The variation in vertical fractures is consistent with that of Well L208, and the concentrated development of horizontal fractures can be found at the top of the 4 sub-layer in the S_1l^1 sub-member (Figure 5). This is associated with the local increase of TOC and interbedding of thin and thick layers, according to the core observation.

5. PETROLOGICAL FACTORS OF FRACTURE DEVELOPMENT

The fracture morphology and development degree are affected by various factors,[45−47] of which the content of brittle minerals and lithofacies are the direct internal factors affecting the development of tectonic fractures.[6,48]

5.1. Mineral Composition and Brittleness Characteristics. Wells L205 and L208 are similar in mineral composition contents and vertical changes (Figure 6). Specifically, the quartz content is ranged from 21 to 74.5%, with 45.5% on average, which reaches the highest in the middle and upper parts of the Wufeng Formation, with decreasing−increasing−decreasing−increasing multimember variations. After this, the quartz content is increased again at the upper parts of the sub-layers 2 and 4. The feldspar content is ranged from 2 to 14%, with 5.4% on average and the maximum reached at the top of sub-layers 2 and 4. The content of clay mineral is ranged from 6 to 46%, with 36% on average, which is increasing vertically. The calcite content is ranged from 6 to 18%, with 8.4% on average and higher contents observed in the middle part of sub-layers 1 and 4 vertically. The pyrite content is ranged from 1 to 8%, with 3.4% on average.

The shale brittleness calculation method based on mineral components is the most commonly used method due to its simple operation and strong applicability. Moreover, quartz, feldspar, and pyrite are characterized by a high elastic modulus and low Poisson's ratio, which are normally considered as brittle minerals.[13,49] Calculation is conducted as follows

$$B_{\mathrm{RIT}} = \{(w_{\mathrm{quartz}} + w_{\mathrm{Feldspar}} + w_{\mathrm{Pyrite}}) / (w_{\mathrm{quartz}} + w_{\mathrm{Feldspar}} + w_{\mathrm{Pyrite}} + w_{\mathrm{carbonate}} + w_{\mathrm{clay}})\} \times 100$$

BRIT is the shale mineral brittleness index, w_{quartz} is the quartz mineral quality fraction, w_{Feldspar} is the feldspar mineral quality fraction; w_{Pyrite} is the pyrite mineral quality fraction; $w_{\mathrm{carbonate}}$ is the carbonate mineral quality fraction; w_{clay} is the clay mineral quality fraction.

According to the calculation results, the brittleness index of the Wufeng−Longmaxi Formation shale in the study area is ranged from 37 to 74.5%, presenting a relatively high level. This indicates that a complex fracture network system is easily formed in the later tectonic movement and fracturing process. Brittleness indexes of different sub-layers in the 1 sub-member of the Longmaxi Formation were changed in the increasing−decreasing−increasing trend. To be concrete, the brittleness index of the Wufeng Formation is ranged from 41.3 to 74.5%, with 48.5% on average; the brittleness index of the 1 sub-layer is ranged from 42.6 to 61.3%, with 50.6% on average; the brittleness index of shale in the 2 sub-layer is ranged from 60 to 74.5%, with 63.6% on average; the brittleness index of shale in the 3 sub-layer is ranged from 55.8 to 61.2%, with 57.3% on average; the brittleness index of the lower member of the 4 sub-layer is ranged from 37 to 53.5%, with 44.2% on average; and the

https://doi.org/10.1021/acsomega.2c03318
ACS Omega 2022, 7, 34066−34079

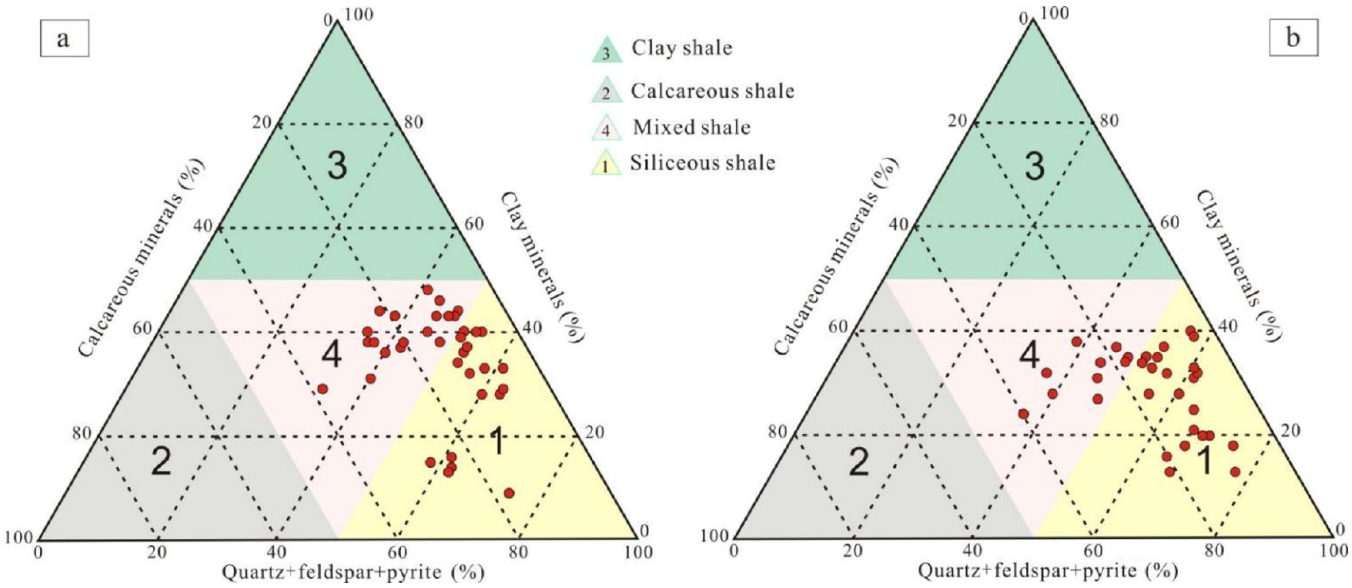

Figure 7. Triangular diagram of relative mineral content and lithofacies classification of Wufeng−Longmaxi Formation shale in Wells Lu (a) 205 and (b) 208.[50]

brittleness index of the upper member is ranged from 38.6 to 58.7%, with 49% on average. There is a good correspondence between shale brittleness and TOC content, and the sample points with TOC content above 2.5% are mainly distributed in siliceous shale facies, according to the TOC content and fracture development distribution at different depths (Figure 7).

5.2. Different Lithofacies Crack Propagation Modes and Crack Development Differences. Different lithofacies are developed vertically at the Wufeng−Longmaxi Formation shale. Meanwhile, bedding fractures are also developed. Different lithofacies interfaces and bedding fractures serve as pre-existing weak surfaces.[51] When the fractures form and expand to these weak surfaces in the later stage, the propagation path of fractures will be deflected to a certain extent, affecting the longitudinal extension of fractures.

Wufeng Formation-1−3 sub-layers of the S_1l^1 sub-member are dominated by extremely organic-rich siliceous shale, with a small amount of calcareous siliceous shale. When the interlaminar fractures are developed in the sub-layer, it might be more likely to rupture in the later tectonic movement. The size of shear resistance is adjusted by siliceous shale particles through the "rotation" of particles under microscopic conditions,[52] which represents a small energy consumption mode that is conducive to the longitudinal expansion of fractures. Fractures, in most cases, break through mineral particles or extend along the mineral contact edge of minerals. The corresponding failure modes of rock mass normally are dominated by "split" and "shear" failures through bedding. There are high-angle or vertical shear fractures appearing on the core, featuring propagation across stratified planes. The brittleness of calcareous siliceous shale is slightly lower than that of siliceous shale. The penetrability of fractures in tectonic movement is weaker than that of siliceous shale. The extended fractures are bent at the lithological interface, especially in development members of interlaminar fracture and horizontal fracture. Moreover, the vertical expansion of fractures leads to a criss-cross phenomenon, while the development of vertical fractures or high-angle fractures is restricted by the upper and lower horizontal fractures, generating I-type or T-type fractures on the plane. Organic-rich siliceous shale and calcareous siliceous shale were developed in the 3 sub-layer of the Wufeng Formation-S_1l^1 sub-member. The thickness of the monolayer is thin. Thin shell limestone is developed on the top surface of the Wufeng Formation. Both horizontal and high-angle fractures are developed. Vertical fractures running through horizontal fractures and vertical fractures restricted by upper and lower horizontal fractures can be observed. High-angle and vertical fractures encounter interlaminar and horizontal fracture interfaces during longitudinal expansion, and complex fracture networks can be developed as the fracture expansion tends to form branches.

Thick organic-poor calcareous siliceous shale is developed at the lower part of the 4 sub-layer, featuring large thickness and a decline in the brittleness of shale, decreased calcareous contents, less developed stratified development, large elastic moduli of shale, high fracture pressure gradients, and high fracture toughness. The longitudinal expansion of fractures is less affected by the "barrier" effect of interlaminar fracture. High-angle and vertical fractures were mainly developed during the tectonic movement, with fewer horizontal fractures developed. Large vertical fractures or high-angle fractures intersecting horizontal fractures can be found in the core, featuring single fracture morphology and low density as a whole. The middle and upper parts of the 4 sub-layer are dominated by clay siliceous shale, with calcareous siliceous shale developed at the same time, and the increased content of clay minerals. Based on the damage mechanism of clay minerals, the fracture propagation caused by stress always starts in the lamellation direction due to the directional arrangement of clay mineral particles. On this basis, fractures characterized by the development of low-angle and horizontal fractures with a small amount of vertical fractures can be caused in the late tectonic movement of clay siliceous shale, which is consistent with the core observation results (Figure 8).

6. EFFECT OF FRACTURE DEVELOPMENT ON GAS-BEARING PROPERTIES

The influence of natural fractures on the gas-bearing properties of shale is demonstrated in promoting shale gas desorption,

https://doi.org/10.1021/acsomega.2c03318
ACS Omega 2022, 7, 34066−34079

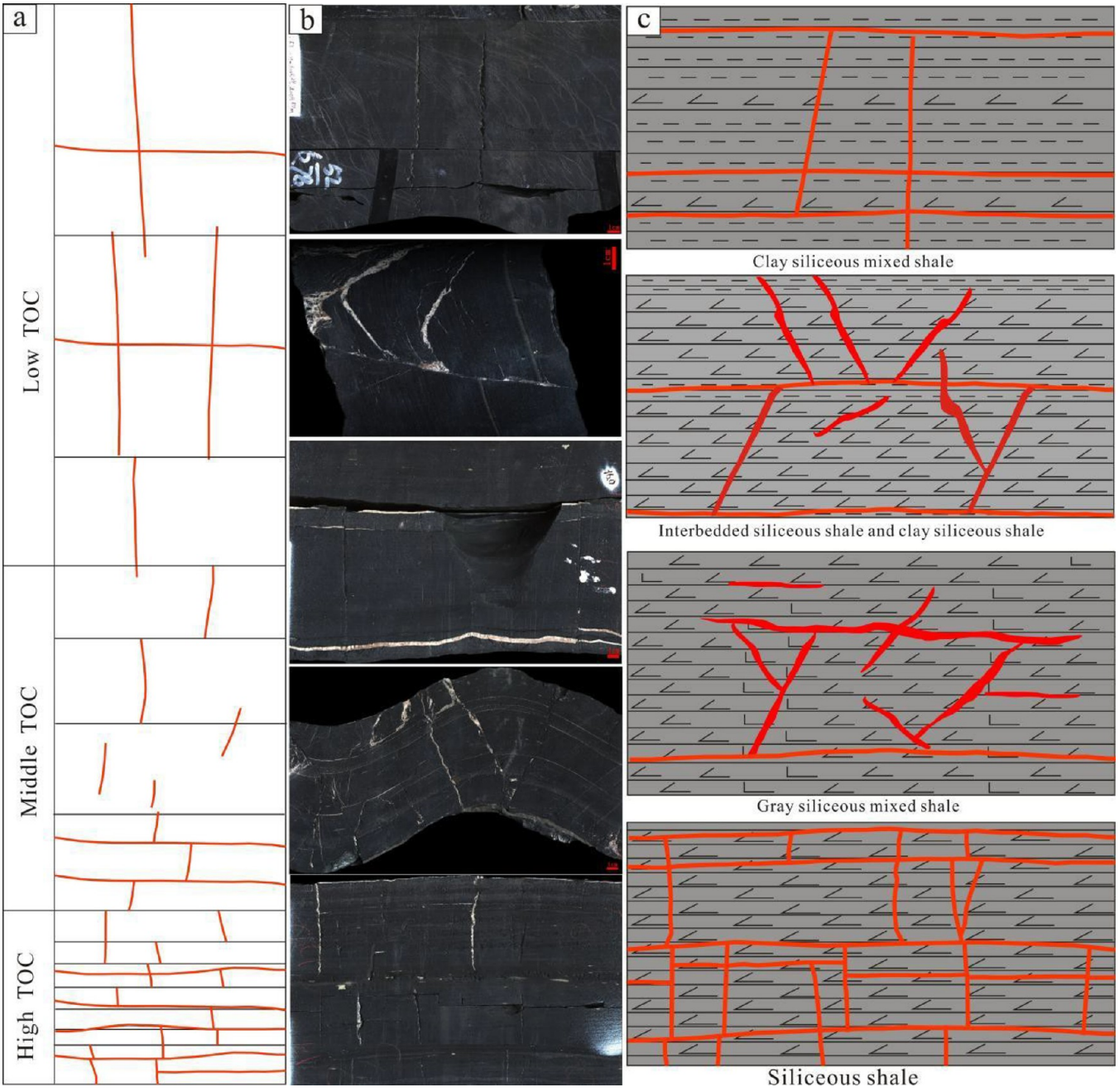

Figure 8. Development and distribution patterns of fractures with different lithologic properties. (a) Longitudinal variation pattern of fractures, (b) performance characteristics of core fractures, and (c) fracture propagation modes of different lithofacies.

migration, accumulation, destruction, and preservation.[53,54] On the one hand, unfilled fractures developed in layers are effective storage spaces for shale gas and conducive to the migration of shale gas.[13,55,56] On the other hand, over-developed fractures might destroy the continuity of roof and bottom plates, resulting in vertical diffusion of shale gas. The hydrocarbon gas formed in shale is adsorbed on the surface of organic matter and mineral particles nearby. The increased pore pressure drives the migration of shale gas to the opened fractures with the continuous formation of shale gas.[57] Fractures as natural pressure release channels contribute to the desorption of adsorbed gas and the increased proportion of free gas.[58] The gas-bearing property of shale is controlled by multiple factors,[59] and a synergistic relationship can be observed among fracture development, organic matter content, and brittleness indices. On the one hand, a large amount of biogenic silicon provided by the sedimentation after the death of low-grade siliceous organisms increases the brittleness of the reservoir and facilitates the development of fractures in the later tectonic movement.[30] Based on the actual shale gas exploration in the Sichuan Basin, the concentrated development member of fractures also witnesses high shale gas-bearing properties, with high TOC contents.[60,61] Moreover, the brittle mineral content, fracture density, and gas-bearing data at different depths in Wells L205 and L208 were statistically analyzed to study the relationship between the degree of fracture development and the gas-bearing property of shale in the Lu203 well area. On this basis, the correlation of brittle mineral contents, fracture density, and gas-bearing data was established, as shown in Figure 9. From which, TOC content, brittle minerals, and shale development density

https://doi.org/10.1021/acsomega.2c03318
ACS Omega 2022, 7, 34066−34079

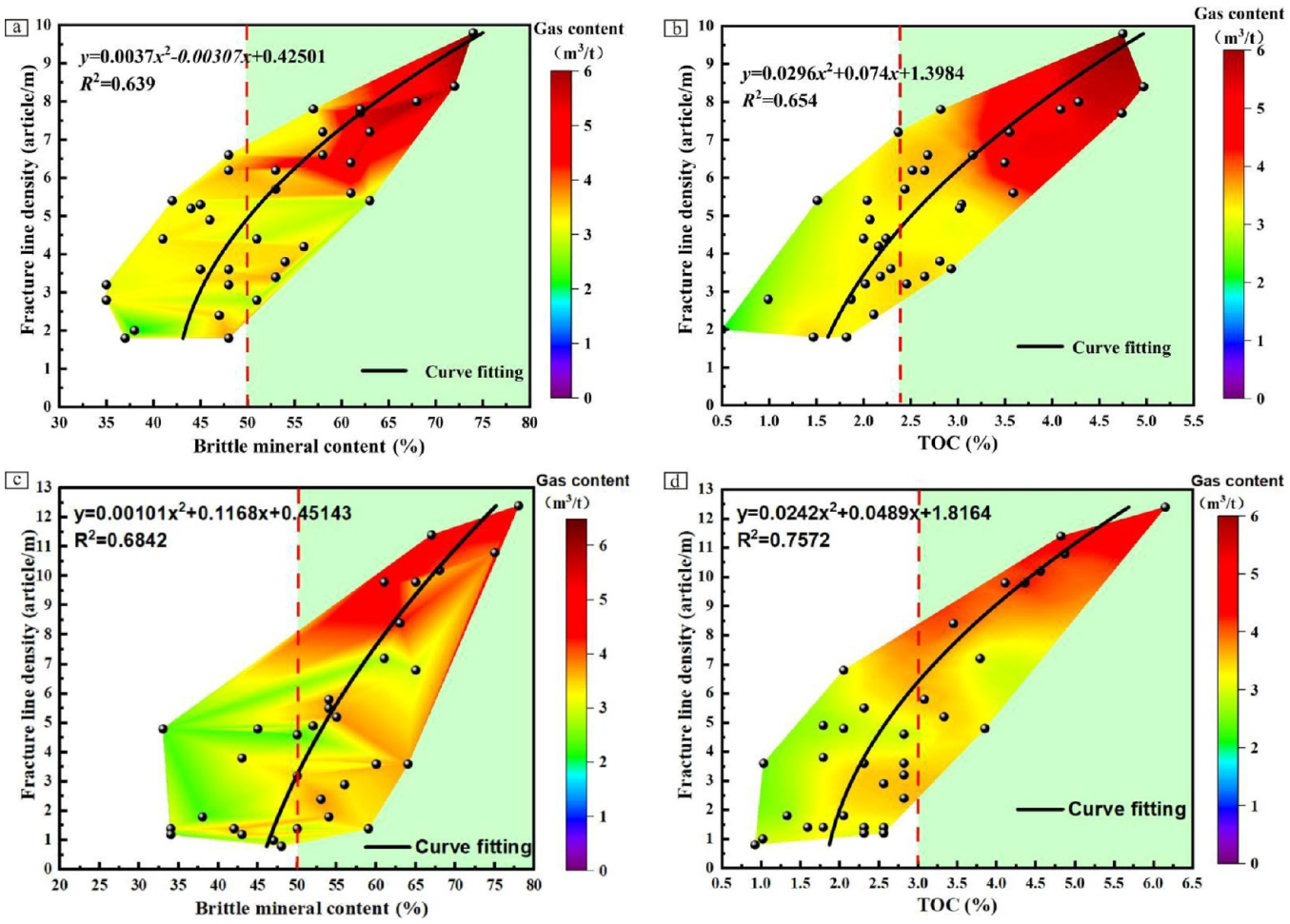

Figure 9. Correlation between shale fracture linear density and brittle mineral−TOC−gas content in Wells (a,b) L205 and (c,d) L208.

have a favorable positive correlation, with the correlation coefficients above 0.65; high gas-bearing properties can be also found in the sample point with high TOC content and shale development density according to the variations in the gas-bearing property of shale at varied statistical members.

The development member of the shale gas reservoir in Well L205 is ranged from 3963.63 to 4040.31 m, with the brittleness index above 55%, stratification developed in large quantity, fairly developed vertical and horizontal fractures. The fractures, in most cases, are filled with minerals and affected by the stratified, horizontal, and vertical fractures, forming a complex network system. The fracture density is above 7 fractures/m. Thick calcareous siliceous shale and clay siliceous shale are developed at the 4 sub-layer, with decreases in contents of organic matters and brittle minerals. Consequently, there are large differences in shale porosity and gas-bearing properties. Specifically, the shale porosity is ranged from 4.15 to 6.41%, with 4.82% on average, and the TOC content is ranged from 0.5 to 4.97%, with 2.65% on average. The total gas content of the shale is calculated to be 4.3 m^3/t, according to log interpretation, with favorably results in the TOC and gas contents of the bottom shale. Fractures in the depth ranging from 4037 to 4042 m in the Wufeng Formation are relatively underdeveloped, with an average porosity of 3.9%, TOC content of 1.6%, free gas content of 1.4 m^3/t, adsorbed gas content of 1.5 m^3/t, and the proportion of free gas less than 50%. Fractures are concentrated at the top member of the Wufeng Formation at the depth ranging from 4034.5 to 4037 m, with a shale content of 3.0 m^3/t and a free gas content of 2.1 m^3/t, accounting for 61.22% of the total gas content. Contents of adsorbed gas and free gas in the 1 sub-layer are 2.4 and 3.6 m^3/t, respectively, both accounting for 60% of the total gas content. Contents of adsorbed gas and free gas in the 2 sub-layer are 2.1 and 3.4 m^3/t, respectively, both accounting for 61.8%. Total contents of the shale in the 3 sub-layer are equivalent to that of the shale in sub-layers, of which contents of adsorbed gas and free gas in the 3 sub-layer are 2.3 and 3.1 m^3/t, respectively, both accounting for 57.4% of the total gas content. The 4 sub-layer is inferior in the overall gas-bearing property and fracture density. Its fracture development has two concentrated members at the top and bottom, which is dominated by horizontal fractures, and a small amount of vertical fractures. The gas content of shale is ranged from 1.8 to 3.8 m^3/t as a whole, with 2.65 m^3/t on average. Specifically, free gas accounts for 54.5%. The average gas content of shale in the development member with concentrated horizontal fractures at the top is 3.16 m^3/t, of which contents of free gas and adsorbed gas are 2.0 and 1.16 m^3/t, respectively, accounting for 63.29% of the total gas content. Nevertheless, the free gas content accounts for roughly 50% of the total gas content in the middle and lower parts of the 4 sub-layer in the underdeveloped member of horizontal fractures. The development degree of fractures is well corresponded with the total gas content of shale and the proportion of free gas content.

https://doi.org/10.1021/acsomega.2c03318
ACS Omega 2022, 7, 34066−34079

The shale gas development member in Well L208 is ranged from 3762.4 to 3851.2 m in depth. Its development distribution law of longitudinal fractures is similar to that of Well L205, with the maximum fracture density observed in the 2 sub-layer. By comparing the differences in gas-bearing properties of different sub-layers, the gas content of Wufeng Formation shale is ranged from 2.34 to 3.66 m^3/t, with 2.48 m^3/t on average. The total gas content of shale in the 1 sub-layer is 4.3 m^3/t, of which the free gas content is 1.6 m^3/t, accounting for 37.2% of the total gas content, with its fracture density of 15.8/m. The total gas content of the shale in the 2 sub-layer is 4.7 m^3/t, of which the free gas content is 2.7 m^3/t, accounting for 57.44%, with its fracture density of 26.4 fractures/m. The total gas content of shale in the 3 sub-layer is 3.6 m^3/t, of which the free gas content is 1.6 m^3/t, accounting for 44.44%, with its fracture density of 3.7 fractures/m. Moreover, the average gas content of the shale in the middle and upper parts of the 4 sub-layer with concentrated fractures is 2.88 m^3/t, of which the free gas content is 1.58 m^3/t, accounting for 54.86%. The fracture density is 1.5 fractures/m. Vertical fractures are highly filled in most cases, whereas horizontal fractures are mostly in a semifilled or open state, according to the observation and statistics of core fracture filling. Hence, the difference in the proportion of free gas content is mainly associated with the development of horizontal fractures. Vertically, TOC content decreases as a whole. The total gas content is decreased in the middle and upper parts of the 4 sub-layer. The proportion of free gas is increased rapidly in the horizontal fracture development member, of which the free gas content is 54.86%. There is a free gas proportion of roughly 57% at the top of the Wufeng Formation and the 2 sub-layer of the Longmaxi Formation with high TOC content and horizontal fractures, whereas the proportion of free gas is below 50% in the middle parts of the 1 and 4 sub-layers with low fracture density of fracture development.

As the shale has a high content of brittle minerals according to the comparison in the fracture development members of the two wells, a favorable gas-bearing property can be observed as a whole. Besides, the horizontal fracture development member at the middle and upper parts of the 4 sub-layer is low in TOC content, causing low shale gas content as a whole. As the unfilled horizontal fractures are relatively developed, favorable conditions are provided for the desorption of adsorbed gas adsorbed on the surface of organic matters and minerals. As a result, there is a rapid increase in the proportion of free gas in the concentrated development of horizontal fractures. Moreover, microfractures on the edge of minerals are relatively developed, which provides conditions for the desorption of shale gas, according to the SEM results. In that case, a large amount of adsorbed gas desorbed into the unfilled fractures is the cause of local enrichment of shale gas in the fracture-developed member and the increased proportion of free gas.

7. CONCLUSIONS

(1) Macrofractures in shale cores of Longmaxi Formation are mainly composed of tectonic fractures, including high-angle-vertical shear fractures, horizontal slip shear fractures, and extension fractures, which account for more than 80% of the total number of fractures. Moreover, nontectonic macrofractures consist of dissolution fractures and abnormally high-pressure fractures. Besides, microfractures are nontectonic fractures, including interlayer fractures, intercrystalline fractures, organic matter contraction fractures, and fractures between clay layers.

(2) Development of core fractures is characterized by short longitudinal extension, small opening, high degrees of composite filling, and large density changes, with calcite and pyrite as the filling materials. The fracture density has a "three-stage" variation pattern longitudinally, and the bottom is dominated by thin siliceous shale development. Its bottom is dominated by thin siliceous shale development. The development of horizontal shear fractures and vertical slipping fracture is developed to form the mesh fracture system through mutual cutting and restriction. The 2 sub-layer witnesses the maximum fracture density, and clay siliceous mixed shale is developed in the 4 sub-layer, which can be found at the top and bottom fracture concentrated development stage, with the horizontal fracture dominated.

(3) What's more, a synergistic and accelerating effect can be found among the TOC content, fracture density, and gas-bearing property of the shale. Note that high TOC content facilitates the sedimentation of high biogenic silicon, jointly contributing to the formation of microfractures. In addition, the development of fractures is highly associated with the shale gas-bearing property, especially with the increase in free gas content, the fast-increasing free gas content proportion in the shale of fracture concentration development members. The fracture provides a channel for the desorption of shale gas, contributing to the accelerated desorption of shale gas and increase in the free gas content.

AUTHOR INFORMATION

Corresponding Author

Qirong Qin − *School of Geoscience and Technology, Southwest Petroleum University, Chengdu 610041, China*; Email: vipheshun001@163.com

Authors

Shun He − *School of Geoscience and Technology, Southwest Petroleum University, Chengdu 610041, China*; orcid.org/0000-0002-5462-7226

Zhangjin Qin − *Exploration Division, Southwest Oil And Gas Field Company, Petro China, Chengdu 610041, China*

Jiling Zhou − *Exploration Division, Southwest Oil And Gas Field Company, Petro China, Chengdu 610041, China*

Complete contact information is available at: https://pubs.acs.org/10.1021/acsomega.2c03318

Notes

The authors declare no competing financial interest.

ACKNOWLEDGMENTS

This research was supported by Open Fund (G5800-20-ZS-KFZY002) of State Key Laboratory of Oil and Gas Enrichment Mechanisms and Effective Development and the National Science and Technology Major Project (2017ZX05036003-003) of the 13th Five-Year Plan Period.

REFERENCES

(1) He, S.; Qin, Q. R.; Li, H.; Wang, S. X. Deformation Differences in Complex Structural Areas in the Southern Sichuan Basin and Its Influence on Shale Gas Preservation: A Case Study of Changning and Luzhou Areas. *Front. Earth Sci.* **2022**, *9*, No. 818534.

(2) Guo, T. L. Key geological issues and main controls on accumulation and enrichment of Chinese shale gas. *Pet. Explor. Dev.* **2016**, *43*, 349−359.
(3) Sun, C. X.; Nie, H. K.; Dang, W.; Chen, Q.; Zhang, G. R.; Li, W. P.; Lu, Z. Y. Shale Gas Exploration and Development in China: Current Status, Geological Challenges, and Future Directions. *Energy Fuels* **2021**, *38*, 6359−6379.
(4) Ma, X. H.; Xie, J.; Yong, R.; Zhu, Y. Q. Geological characteristics and high production control factors of shale gas reservoirs in Silurian Longmaxi Formation, southern Sichuan Basin, SW China. *Pet. Explor. Dev.* **2020**, *47*, 901−915.
(5) Wang, R. Y.; Hu, Z. Q.; Long, S. X.; Liu, G. X.; Zhao, J. H.; Dong, L.; Du, W.; Wang, P. W.; Yin, S. Differential Characteristics of the Upper Ordovician-Lower Silurian Wufeng-Longmaxi Shale Reservoir and its Implications for Exploration and Development of Shale Gas in/around the Sichuan Basin. *Acta Geol. Sin.* **2019**, *93*, 520−535.
(6) He, S.; Li, H.; Qin, Q. R.; Long, S. X. Influence of Mineral Compositions on Shale Pore Development of Longmaxi Formation in the Dingshan Area, Southeastern Sichuan Basin, China. *Energy Fuels* **2021**, *35*, 10551−10561.
(7) Yang, F.; Ning, Z. F.; Wang, Q.; Zhang, R.; Krooss, B. M. Pore structure characteristics of lower Silurian shales in the southern Sichuan Basin, China: Insights to pore development and gas storage mechanism. *Int. J. Coal Geol.* **2016**, *156*, 12−24.
(8) Li, Y.; Zhou, D. H.; Wang, W. H.; Jiang, T. X.; Xue, Z. J. Development of unconventional gas and technologies adopted in China. *Energy Geosci.* **2020**, *1*, 55−68.
(9) Bakshi, T.; Vishal, V. A Review on the Role of Organic Matter in Gas Adsorption in Shale. *Energy Fuels* **2021**, *35*, 15249−15264.
(10) Li, Y.; Chen, S. J.; Qiu, W.; Su, K. M.; Wu, B. Y. Controlling factors for the accumulation and enrichment of tight sandstone gas in the Xujiahe Formation, Guang'an Area, Sichuan Basin. *Energy Explor. Exploit.* **2019**, *37*, 26−43.
(11) Tan, P.; Jin, Y.; Han, K.; Hou, B.; Chen, M.; Guo, X. F.; Gao, J. Analysis of hydraulic fracture initiation and vertical propagation behavior in laminated shale formation. *Fuel* **2017**, *206*, 482−493.
(12) Liu, B.; Sun, J. H.; Zhang, Y. Q.; He, J. L.; Fu, X. F.; Yang, L.; Xing, J. L.; Zhao, X. Q. Reservoir space and enrichment model of shale oil in the first member of Cretaceous Qingshankou Formation in the Changling Sag, southern Songliao Basin, NE China. *Pet. Explor. Dev.* **2021**, *48*, 608−624.
(13) Li, J.; Li, H.; Yang, C.; Wu, Y. J.; Gao, Z.; Jiang, S. L. Geological characteristics and controlling factors of deep shale gas enrichment of the Wufeng-Longmaxi Formation in the southern Sichuan Basin, China. *Lithosphere* **2022**, *2022*, No. 4737801.
(14) Sheng, Y.; Sousani, M.; Ingham, D.; Pourkashanian, M. Recent developments in multiscale and multiphase modelling of the hydraulic fracturing process. *Math. Probl. Eng.* **2015**, 1.
(15) Gu, Y.; Ding, W. L.; Tian, Q. N.; Xu, S.; Zhang, W.; Zhang, B. R.; Jiao, B. C. Developmental characteristics and dominant factors of natural fractures in lower Silurian marine organic-rich shale reservoirs: A case study of the Longmaxi formation in the Fenggang block, southern China. *J. Pet. Sci. Eng.* **2020**, *192*, No. 107277.
(16) Li, Y. F.; Sun, W.; Liu, X. W.; Zhang, D. W.; Wang, Y. C.; Liu, Z. Y. Study of the relationship between fractures and highly productive shale gas zones, Longmaxi Formation, Jiaoshiba area in eastern Sichuan. *Pet. Sci.* **2018**, *15*, 498−509.
(17) Li, X. M.; Wang, Y. R.; Lin, W.; Ma, L. H.; Liu, D. X.; Zhang, Y. Tectonic Characteristics and its Effect on Shale Gas Preservation Condition in the Jingmen Region. *Front. Earth Sci.* **2022**, *9*, No. 821593.
(18) Gao, F. Q. Use of numerical modeling for analyzing rock mechanic problems in underground coal mine practices. *J. Min. Strata Control Eng.* **2019**, *1*, No. 013004.
(19) Li, H. T.; Peng, R.; Du, W. S.; Li, X. P.; Zhang, N. B. Experimental study on structural sensitivity and intervention mechanism of mechanical behavior of coal samples. *J. Min. Strata Control Eng.* **2021**, *3*, No. 043012.
(20) Qie, L.; Shi, Y. N.; Liu, J. G. Experimental study on grouting diffusion of gangue solid filling bulk materials. *J. Min. Strata Control Eng.* **2021**, *3*, No. 023011.
(21) Liang, X.; Hou, P.; Xue, Y.; Yang, X. J.; Gao, F.; Liu, J. A Fractal Perspective on Fracture initiation and Propagation of Reservoir Rocks Under Water and Nitrogen Fracturing. *Fractals* **2021**, *29*, No. 215018.
(22) Jiang, T. X.; Zhou, J.; Zhang, X.; Hou, L.; Xiao, B. Overview and prospect of fracture propagation and conductivity characteristics in deep shale gas wells. *Sci. Sin. Phys., Mech. Astron.* **2017**, *47*, 114603.
(23) Wu, K.; Olson, J. E. Simultaneous multifracture treatments: fully coupled fluid flow and fracture mechanics for horizontal wells. *SPE J.* **2015**, *20*, 337−346.
(24) Li, S. J.; Li, Y. Q.; He, Z. L.; Chen, K.; Zhou, Y.; Yan, D. T. Differential deformation on two sides of Qiyueshan Fault along the eastern margin of Sichuan Basin, China, and its influence on shale gas preservation. *Mar. Pet. Geol.* **2020**, *121*, No. 104602.
(25) Gale, J. F. W.; Laubach, S. E.; Olson, J. E.; Eichhubl, P.; Fall, A. Natural fractures in shale: A review and new observations. *AAPG Bull.* **2014**, *98*, 2165−2216.
(26) Li, H.; Wang, Q.; Qin, Q. R.; Ge, X. Y. Characteristics of natural fractures in an ultradeep marine carbonate gas reservoir and their impact on the reservoir: A case study of the Maokou Formation of the JLS Structure in the Sichuan Basin, China. *Energy Fuels* **2021**, *35*, 13098−13108.
(27) Kim, T. H.; Lee, K. S. Pressure-Transient Characteristics of Hydraulically Fractured Horizontal Wells in Shale-Gas Reservoirs With Natural- and Rejuvenated-Fracture Networks. *J. Can. Pet. Technol.* **2015**, *54*, 245−258.
(28) Zhang, X. M.; Shi, W. Z.; Hu, Q. H.; Zhai, G. Y.; Wang, R.; Xu, X. F.; Meng, F. L.; Liu, Y. Z.; Bai, L. H. Developmental characteristics and controlling factors of natural fractures in the lower paleozoic marine shales of the upper Yangtze Platform, southern China. *J. Nat. Gas Sci. Eng.* **2020**, *76*, No. 103191.
(29) Zhou, T.; Zhang, S. C.; Feng, Y.; Shuai, Y. Y.; Zou, Y. S.; Li, N. Experimental study of permeability characteristics for the cemented natural fractures of the shale gas formation. *J. Nat. Gas Sci. Eng.* **2016**, *29*, 345−354.
(30) He, S.; Qin, Q. R.; Li, H.; Zhao, S. X. Geological Characteristics of Deep Shale Gas in the Silurian Longmaxi Formation in the Southern Sichuan Basin, China. *Front. Earth Sci.* **2022**, *9*, No. 818155.
(31) Li, H. Research progress on evaluation methods and factors influencing shale brittleness: A review. *Energy Rep.* **2022**, *8*, 4344−4358.
(32) Hu, X. T.; Chen, L.; Qi, L.; Lei, Z. A.; Luo, Y. Marine shale reservoir evaluation in the Sichuan Basin-A case study of the Lower Silurian Longmaxi marine shale of the B201 well in the Baoluan area, southeast Sichuan Basin, China. *J. Pet. Sci. Eng.* **2019**, *182*, No. 106339.
(33) Liu, S. G.; Deng, B.; Li, Z. W.; Sun, W. Architecture of basin-mountain systems and their influences on gas distribution: A case study from the Sichuan basin, South China. *J. Asian Earth Sci.* **2012**, *47*, 204−215.
(34) Guo, X. S.; Li, Y. P.; Borjigen, T.; Wang, Q.; Yuan, T.; Shen, B. J.; Ma, Z. L.; Wei, F. B. Hydrocarbon generation and storage mechanisms of deep-water shelf shales of Ordovician Wufeng Formation−Silurian Longmaxi Formation in Sichuan Basin, China. *Pet. Explor. Dev.* **2020**, *47*, 204−213.
(35) Ma, X. H.; Xie, J. The progress and prospects of shale gas exploration and exploitation in southern Sichuan Basin, SW China. *Pet. Explor. Dev.* **2020**, *45*, 172−182.
(36) He, L.; Wang, Y. P.; Chen, D. F. Geochemical features of sedimentary environment and paleoclimate during Late Ordovician to Early Silurian in southern Sichuan Basin. *Geochimica* **2019**, *48*, 555−566.
(37) Guo, W. X.; Tang, J. M.; Ouyang, J. H.; Wang, T.; Wang, X.; Wang, Y. Characteristics of structural deformation in the southern Sichuan Basin and its relationship with the storage condition of shale gas. *Nat. Gas Ind.* **2021**, *41*, 11−19.
(38) Pu, B. L.; Dong, D. Z.; Ning, X. J.; Wang, S. F.; Wang, Y. M.; Feng, S. K. Lithology and sedimentary heterogeneity of Longmaxi shale in the southern Sichuan Basin. *Interpretation* **2022**, *10*, T45−T56.

https://doi.org/10.1021/acsomega.2c03318
ACS Omega 2022, 7, 34066−34079

(39) Zou, C. N.; Dong, D. Z.; Wang, Y. M.; Li, X. J.; Huang, J. L.; Wang, S. F.; Guan, Q. Z.; Zhang, C. C.; Wang, H. Y.; Liu, H. L.; Bai, W. H.; Liang, F.; Lin, W.; Zhao, Q.; Liu, D. X.; Yang, Z.; Liang, P. P.; Sun, S. S.; Qiu, Z. Shale gas in China: characteristics, challenges and prospects(II). *Pet. Explor. Dev.* **2016**, *43*, 182−196.
(40) Kong, X. Y.; Zeng, J. H.; Tan, X. F.; Ding, K.; Luo, Q.; Wang, Q. Y.; Wen, M.; Wang, X.; Wang, M. Y. Natural tectonic fractures and their formation stages in tight reservoirs of Permian Lucaogou Formation, Jimsar Sag, southern Junggar Basin, NW China. *Mar. Pet. Geol.* **2021**, *133*, No. 105269.
(41) Curtis, J. B. Fractured shale-gas systems. *AAPG Bull.* **2002**, *86*, 1921−1938.
(42) Li, H.; Tang, H. M.; Zheng, M. J. Micropore Structural Heterogeneity of Siliceous Shale Reservoir of the Longmaxi Formation in the Southern Sichuan Basin, China. *Minerals* **2019**, *9*, 548.
(43) Li, H.; Tang, H. M.; Qin, Q. R.; Wang, Q.; Zhong, C. Effectiveness evaluation of natural fractures in Xujiahe Formation of Yuanba area, Sichuan basin, China. *Arabian J. Geosci.* **2019**, *12*, 194.
(44) Ding, W. L.; Xu, C. C.; Jiu, K.; Li, C.; Zeng, W. T.; Wu, L. M. The Research Progress and Shale Fractures. *Adv. Earth Sci.* **2011**, *26*, 135−144.
(45) Ding, W. L.; Li, C.; Li, C. H.; Jiu, K.; Zeng, W. T. Dominant factor of fracture development in shale and its relationship to gas accumulation. *Earth Sci. Front.* **2012**, *19*, 212−220.
(46) Li, H.; Tang, H. M.; Qin, Q. R.; Zhou, J. L.; Qin, Z. J.; Fan, C. H.; Su, P. D.; Wang, Q.; Zhong, C. Characteristics, formation periods and genetic mechanisms of tectonic fractures in the tight gas sandstones reservoir: A case study of Xujiahe Formation in YB area, Sichuan Basin, China. *J. Pet. Sci. Eng.* **2019**, *178*, 723−735.
(47) Fan, C. H.; Xie, H. B.; Li, H.; Zhao, S. X.; Shi, X. C.; Liu, J. F.; Meng, L. F.; Hu, J.; Lian, C. B. Complicated fault characterization and its influence on shale gas preservation in the southern margin of the Sichuan Basin, China. *Lithosphere* **2022**, *2022*, No. 8035106.
(48) Fan, C. H.; Li, H.; Qin, Q. R.; He, S.; Zhong, C. Geological conditions and exploration potential of shale gas reservoir in Wufeng and Longmaxi Formation of southeastern Sichuan Basin, China. *J. Pet. Sci. Eng.* **2020**, *191*, No. 107138.
(49) Curtis, M. E.; Cardott, B. J.; Sondergeld, C. H.; Rai, C. S. Development of organic porosity in the Woodford Shale with increasing thermal maturity. *Int. J. Coal Geol.* **2012**, *103*, 26−31.
(50) Wang, Y. M.; Wang, S. F.; Dong, D. Z.; Li, X. J.; Huang, J. L.; Zhang, C. C.; Guan, Q. Z. Lithofacies characterization of Longmaxi Formation of the Lower Silurion, southern Sichuan. *Earth Sci. Front.* **2016**, *23*, 119−133.
(51) Ming, Y. H.; Hutchinson, J. W. Crack deflection at an interface between dissimilar elastic materials. *Int. J. Solids Struct.* **1989**, *25*, 1053−1067.
(52) Rahimzadeh, K. I.; Ameri, M.; Molladavoodi, H. Shale brittleness evaluation based on energy balance analysis of stress-strain curves. *J. Pet. Sci. Eng.* **2018**, *167*, 1−19.
(53) Shen, C.; Ren, L.; Zhao, J. Z.; Tan, X. C.; Wu, L. Z. A comprehensive evaluation index for shale reservoirs and its application: A case study of the Ordovician Wufeng Formation to Silurian Longmaxi Formation in southeastern margin of Sichuan Basin, SW China. *Pet. Explor. Dev.* **2017**, *44*, 686−695.
(54) Han, S. B. A.; Zhang, J. C.; Yang, C.; Bai, S. T.; Huang, L. X.; Dang, W.; Wang, C. S. Well log evaluation of shale gas reservoirs and preservation conditions of Lower Cambrian shale succession in Cengong Block of southeast Sichuan basin, south China. *J. Nat. Gas Sci. Eng.* **2016**, *33*, 337−346.
(55) Ma, Y. Z.; Wang, M.; Ma, R. Y.; Li, J. M.; Bake, A.; Shan, Y. D. Micropore Characteristics and Gas-Bearing Characteristics of Marine-Continental Transitional Shale Reservoirs in the East Margin of Ordos Basin. *Adsorpt. Sci. Technol.* **2021**, *2021*, No. 5593245.
(56) Shi, Z. S.; Dong, D. Z.; Wang, H. Y.; Sun, S. S.; Wu, J. Reservoir characteristics and genetic mechanisms of gas-bearing shales with different laminae and laminae combinations: A case study of Member 1 of the Lower Silurian Longmaxi shale in Sichuan Basin, SW China. *Pet. Explor. Dev.* **2020**, *47*, 888−900.
(57) Yao, J.; Song, W. H.; Li, Y.; Sun, H.; Yang, Y. F.; Zhang, L. Study on the influence of organic pores on shale gas flow ability. *Synth. React. Inorg., Met.-Org., Nano-Met. Chem.* **2017**, *47*, No. 09470.
(58) Wang, Y.; Liu, L. F.; Cheng, H. F. Gas Adsorption Characterization of Pore Structure of Organic-rich Shale: Insights into Contribution of Organic Matter to Shale Pore Network. *Nat. Resour. Res.* **2021**, *30*, 2377−2395.
(59) Sun, J.; Xiao, X. M.; Wei, Q.; Cheng, P.; Tian, H. Occurrence of Irreducible Water and Its Influences on Gas-Bearing Property of Gas Shales From Shallow Longmaxi Formation in the Xishui Area, Guizhou, Southern China. *Earth Sci. Front.* **2021**, *9*, No. 654136.
(60) Jing, T. Y.; Zhang, J. C.; Xu, S. S.; Liu, Z. J.; Han, S. B. Critical geological characteristics and gas-bearing controlling factors in Longmaxi shales in southeastern Chongqing, China. *Energy Explor. Exploit.* **2016**, *34*, 42−60.
(61) Pan, X. P.; Zhang, G. Z.; Chen, J. J. The construction of shale rock physics model and brittleness prediction for high-porosity shale gas-bearing reservoir. *Pet. Sci.* **2020**, *17*, 658−670.

https://doi.org/10.1021/acsomega.2c03318
ACS Omega 2022, 7, 34066−34079